





Article

The Aromatic Head Group of Spider Toxin Polyamines Influences Toxicity to Cancer Cells

David Wilson ¹, Glen M. Boyle ² , Lachlan McIntyre ³, Matthew J. Nolan ¹ , Peter G. Parsons ² , Jennifer J. Smith ⁴, Leon Tribolet ¹, Alex Loukas ¹, Michael J. Liddell ³, Lachlan D. Rash ^{4,5}  and Norelle L. Daly ^{1,*}

¹ Centre for Biodiscovery and Molecular Development of Therapeutics, AITHM, James Cook University, Cairns, QLD 4878, Australia; david.wilson4@jcu.edu.au (D.W.); mjnolan78@gmail.com (M.J.N.); leon.tribolet@gmail.com (L.T.); alex.loukas@jcu.edu.au (A.L.)

² QIMR Berghofer Medical Research Institute, Herston, QLD 4006, Australia; Glen.Boyle@qimrberghofer.edu.au (G.M.B.); Peter.Parsons@qimr.edu.au (P.G.P.)

³ Centre for Tropical Environmental and Sustainable Sciences, James Cook University, Cairns, QLD 4878, Australia; lach.mcintyre@gmail.com (L.M.); michael.liddell@jcu.edu.au (M.J.L.)

⁴ Institute for Molecular Bioscience, The University of Queensland, Brisbane, QLD 4072, Australia; jennifer.smith@imb.uq.edu.au (J.J.S.); l.rash@uq.edu.au (L.D.R.)

⁵ School of Biomedical Sciences, University of Queensland, Brisbane, QLD 4072, Australia

* Correspondence: norelle.daly@jcu.edu.au; Tel.: +61-7-4232-1815

Academic Editor: Hang Fai (Henry) Kwok

Received: 5 September 2017; Accepted: 23 October 2017; Published: 27 October 2017

Abstract: Spider venoms constitute incredibly diverse libraries of compounds, many of which are involved in prey capture and defence. Polyamines are often prevalent in the venom and target ionotropic glutamate receptors. Here we show that a novel spider polyamine, PA₃₆₆, containing a hydroxyphenyl-based structure is present in the venom of several species of tarantula, and has selective toxicity against MCF-7 breast cancer cells. By contrast, a polyamine from an Australian funnel-web spider venom, which contains an identical polyamine tail to PA₃₆₆ but an indole-based head-group, is only cytotoxic at high concentrations. Our results suggest that the ring structure plays a role in the cytotoxicity and that modification to the polyamine head group might lead to more potent and selective compounds with potential as novel cancer treatments.

Keywords: spider venom; NMR spectroscopy; polyamine; cancer; cytotoxicity

1. Introduction

The discovery of new compounds from nature is still one of the most efficient methods for finding lead molecules for the development of pharmaceuticals [1,2]. These new compounds range from small molecules to large biologics, and several approaches have facilitated their discovery. Screening using NMR spectroscopy and recent advances in metabolomics have been valuable for characterising novel small molecules, whereas advances in genomics and proteomics, as well as high-throughput screening approaches are providing novel methods for the discovery of peptides and proteins [3,4].

In nature, venomous creatures are a rich source of new bioactive compounds. In particular, spider venoms have enormous compound diversity, much of which has yet to be explored. More than four million compounds are estimated to be present in the venom of the 46,000 different spider species [5,6]. Spider venom components are present for prey capture and defence purposes; however, some venom compounds have been shown to have therapeutic potential, such as in the treatment of pain and inflammation [7]. While the majority of compounds present in spider venoms are disulfide-rich

peptides [5], small molecules such as the sulfated nucleosides found in brown recluse spiders [8] and polyamines, found in many spider species (reviewed in [9]), are also present.

Polyamines are cationic compounds widespread throughout nature and are found in both prokaryotic and eukaryotic organisms. They can modulate a range of cellular processes that include cell proliferation, signalling and ion channel function [10]. The biological activities of polyamines are mediated through interaction with anionic molecules including DNA, RNA and proteins. However, such structural diversity exists amongst the polyamines that some have been shown to be involved in tumorigenesis [11], and some have shown potential in treating diseases such as cancer [12]. Polyamines with potential for treating diseases include examples from marine sponges and fungi that inhibit carbonic anhydrase IX, a cancer drug target [13]. One study that showed the conjugation of certain polyamines to chloramphenicol enhanced anti-cancer and anti-bacterial activity [14]. The polyamine toxins present in spider venoms are part of a sub-class of polyamines characterised by an aromatic head group with a polyamine chain that can block ionotropic glutamate (iGlu) receptors [12,15]. These receptors have been considered as promising drug targets for neurological and psychiatric disorders [16].

Using a combination of NMR and bioassay screening, we have identified and characterised a novel polyamine (PA₃₆₆) present in a range of tarantula (Theraphosidae) venoms. PA₃₆₆ contains a hydroxyphenyl-based aromatic head group and has more potent cytotoxicity against MCF-7 breast cancer cells than SK-MEL-28 melanoma or neonatal foreskin fibroblast (NFF) primary cells. Potential protein binding interactions were probed using protein array analysis to investigate the mechanism of action, and a comparison with an indole-based polyamine from Australian funnel-web spider venom provided insight into the structure/function relationships.

2. Results

2.1. Cytotoxicity Assays and Characterisation of Bioactive Compound

Crude venoms from female specimens of 31 species of tarantula (Theraphosidae) were screened for activity against the MCF-7 breast cancer cell line. Crude venom from funnel web spiders (male Sydney Funnel-web spider (*Atrax robustus*), female *Hadronyche valida*, *Hadronyche cerbera* and *Hadronyche infensa*- including species variants), and the wolf spider *Hogna carolinensis*, was also tested to allow comparison with venom from two other families (Hexathelidae and Lycosidae). Substantial cytotoxicity activity (defined as greater than 50% decrease in absorbance relative to the negative control) was observed for 17 of the species tested including examples from all three families tested (see Table S1 for the complete list of species screened). The cytotoxicity observed with crude female *Phlogius* sp. spider venom is shown in Figure 1A.

Venom from eight species that displayed cytotoxicity were chosen for further study based on availability of sample, and are listed in Table 1. Crude venom from these eight species were fractionated using reversed-phase high performance liquid chromatography (RP-HPLC), and one-minute fractions were collected. The fractions were subsequently tested against two cancer cell lines, MCF-7 and SK-MEL-28 cells (melanoma cell line) in a clonogenic-type assay. These cell lines were chosen to cover different origins of cancer as MCF-7 are epithelial based and the SK-MEL-28 cells are from neural crest. NFF cells were also tested to represent normal cells with a doubling time similar to cancer cell lines. Variation was observed in activity between the fractionated venoms, and is consistent with venom component variations between spiders as shown previously for related species [5,17]. Despite this variation, all eight species showed early eluting fractions in the RP-HPLC chromatograms that demonstrated activity against the MCF-7 breast cancer cell line.

HSQC-TOCSY spectra, and coupling constants and chemical shifts measured from one-dimensional ^1H NMR spectra. The multiplicities of the ^1H NMR signals are reported as: d, doublet; t, triplet; p, pentet; m, multiplet; br, broad. Coupling constants (J values) are reported in hertz (Hz). HRMS: calculated for $\text{C}_{19}\text{H}_{34}\text{N}_4\text{O}_3$ $[\text{M} + \text{H}]^+$ 367.2631, found 367.2653. ^1H NMR (600 MHz, $\text{H}_2\text{O}/10\% \text{D}_2\text{O}$): δ 8.06 (1H, br t, $J = 6.21$ Hz, H_s), 7.16 (2H, d, $J = 8.71$ Hz, H_b), 6.85 (2H, d, $J = 8.71$ Hz, H_a), 4.41 (1H, t, $J = 5.96$ Hz, H_d), 3.31–3.25 (2H, m, H_e), 3.20–3.08 (6H, m, $\text{H}_n, \text{H}_h, \text{H}_i$), 3.02–2.93 (4H, m, H_c, H_k), 2.73 (2H, br t, $J = 8.72$ Hz, H_g), 2.08 (2H, br p, H_m), 1.78–1.71 (6H, br m, $\text{H}_j, \text{H}_l, \text{H}_f$). ^{13}C NMR (150 MHz, $\text{H}_2\text{O}/10\% \text{D}_2\text{O}$): δ 179.0, 156.7, 133.3 (2C), 130.7, 118.3 (2C), 73.7, 48.8, 48.6, 46.7, 46.2, 40.4, 38.4, 37.4, 27.1, 25.5, 24.3 (2C). The proton assignments are displayed on the one-dimensional spectrum in Figure 3. MS/MS fragmentation resulted in two primary fragment ions of m/z 129.26 and m/z 293.37, consistent with fragmentation at the sites labelled in Figure 2B. Other fragment ions were also evident including m/z 58.15, m/z 112.23 and m/z 222.28, and are consistent with the fragmentation patterns observed in similar molecules [18]. The theoretical calculated mass for the derived structure of PA_{366} is 366.2631 Da, and a m/z 367.2653 (exact mass 366.2573 Da) was observed by MALDI-MS in reflector positive ion mode.

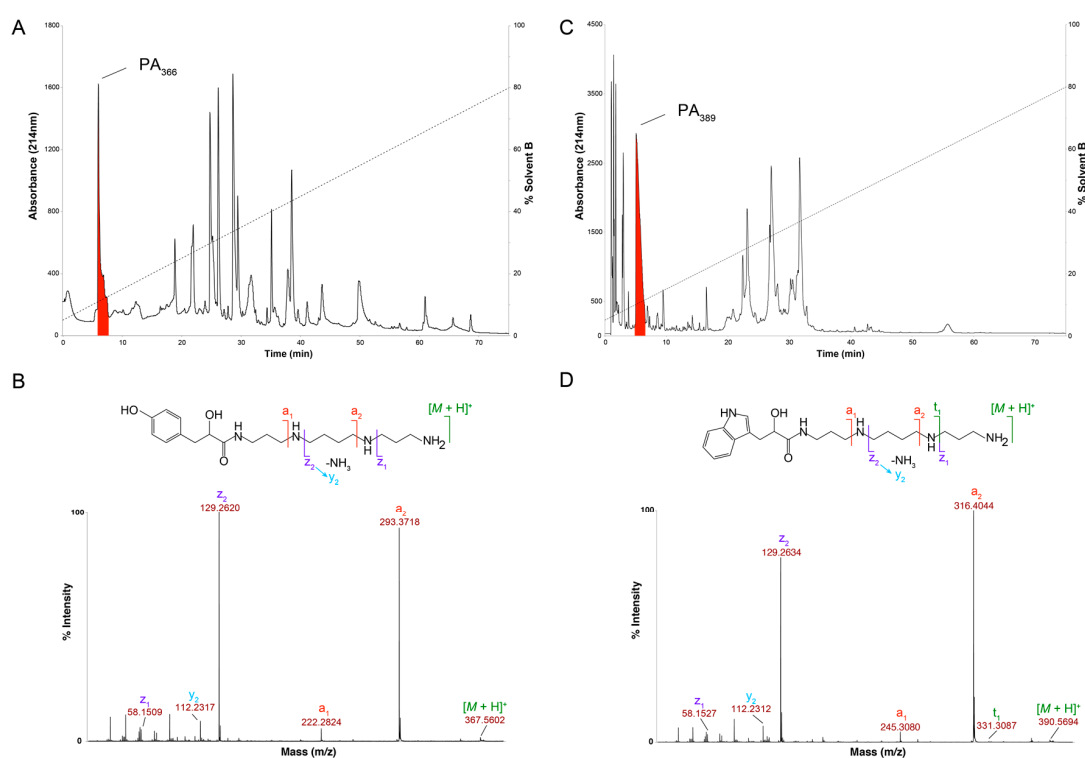


Figure 2. Characterisation of spider venom polyamines. (A) RP-HPLC chromatogram of crude female *Phlogius* sp. venom with the peak corresponding to the polyamine PA_{366} highlighted in red (Thermo Scientific Hypersil GOLD aQ 250×10 mm, $5 \mu\text{m}$ column; $1 \text{ mL}/\text{min}$ flow rate; Solvent A $\text{H}_2\text{O}/0.05\% \text{ TFA}$, Solvent B $90\% \text{ ACN}/\text{H}_2\text{O}/0.045\% \text{ TFA}$; 5–80% solvent B in 75 min, 80–90% solvent B in 5 min, 90% solvent B for 5 min, and 90–5% solvent B in 2 min; absorbance at 214 nm); (B) SCIEX TOF/TOFTM 5800 MALDI MS/MS spectrum of PA_{366} using CHCA matrix, and the determined chemical structure with relevant fragment ions highlighted; (C) RP-HPLC chromatogram of crude female *A. robustus* venom with the peak corresponding to the polyamine PA_{389} highlighted in red (Thermo Scientific Hypersil GOLD aQ 250×10 mm, $5 \mu\text{m}$ column; $1 \text{ mL}/\text{min}$ flow rate; Solvent A $\text{H}_2\text{O}/0.05\% \text{ TFA}$, Solvent B $90\% \text{ ACN}/\text{H}_2\text{O}/0.045\% \text{ TFA}$; 5–80% solvent B in 75 min, 80–90% solvent B in 5 min, 90% solvent B for 5 min, and 90–5% solvent B in 2 min; absorbance at 214 nm); (D) SCIEX TOF/TOFTM 5800 MALDI-MS/MS spectrum of PA_{389} using CHCA matrix, and the determined chemical structure with relevant fragment ions highlighted.

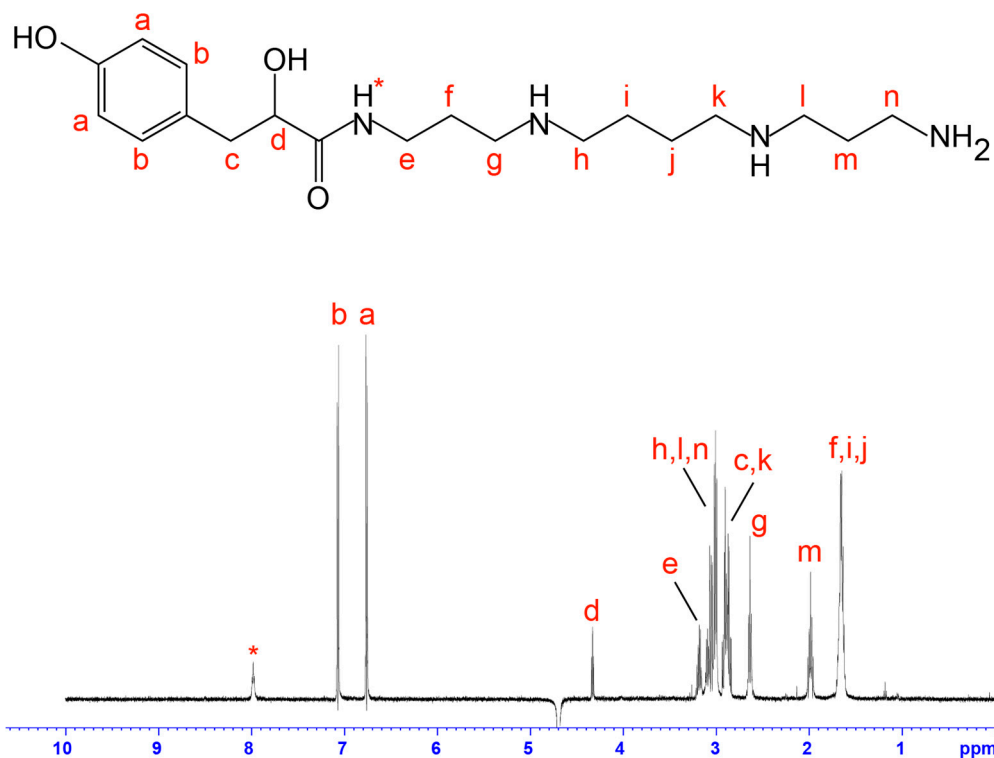


Figure 3. Chemical structure and ^1H NMR spectrum of PA_{366} . The assignments were derived based on two-dimensional NMR spectra and confirmed using mass spectrometry fragmentation analysis.

2.2. NMR Screening of Crude Spider Venoms

Following the characterisation of purified PA_{366} , crude venom from the seven other spiders that showed early eluting fractions with cytotoxic activity were analysed using one-dimensional NMR spectroscopy to screen for the presence of PA_{366} . The one-dimensional NMR spectra of selected examples are shown in Figure 4. Although spider venoms have numerous disulfide-rich peptides, the small molecules have sharper peaks in the 1D spectra, making them easily discernible from peptide signals. This analysis confirmed the presence of PA_{366} in the crude venom from the spider species *Acanthoscuria geniculata*, *Chilobrachys penang*, and *Psalmopoeus irminia*, in addition to the *Phlogius* sp.

Analysis of the NMR spectra of the crude venom of *Ceratogyrus darlingi* and *A. robustus* indicated they do not contain PA_{366} , despite demonstrating cytotoxic activity in the assays. The lack of PA_{366} was confirmed by mass spectrometry analysis, and instead a mass of 389 Da was present. The structure of this active component in *A. robustus* venom was determined following further purification by RP-HPLC, and subsequent analysis using NMR spectroscopy and MS/MS. The analysis determined that *A. robustus* venom contains a polyamine previously characterised from the venom of a trap-door spider (*Hebestatis theveniti*) and a tarantula (*Harpactirella* sp.), and termed Het_{389} [19]. Subsequent analysis of the *C. darlingi* venom also confirmed the presence of Het_{389} . Given the presence of Het_{389} across multiple genera, we suggest the new identifying term PA_{389} is more appropriate. The structure of PA_{389} is shown in Figure 2D and the 1D NMR spectra in Figure 4. The theoretical calculated exact mass for PA_{389} is 389.2791 Da, and a m/z 390.2443 (exact mass 389.2364 Da) was observed by MALDI-MS in reflector positive ion mode. In comparison to the hydroxyphenyl based head group in PA_{366} , PA_{389} has an indole head group and identical spermine tail. The cytotoxicity of PA_{389} is shown in Figure 5 and shows this polyamine only displays cytotoxicity at millimolar concentrations.

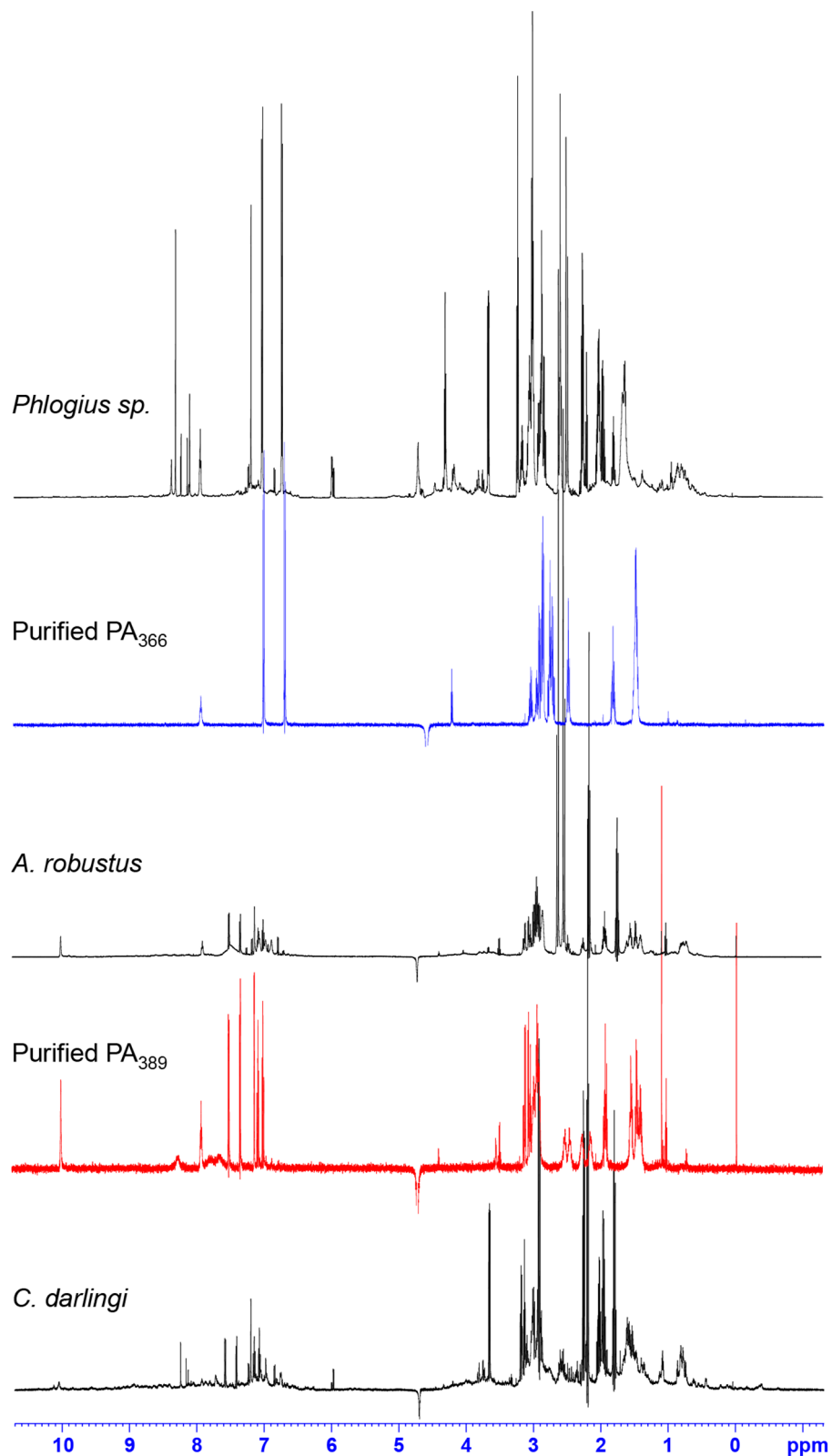


Figure 4. One-dimensional NMR spectra of selected crude spider venoms and purified polyamines. ^1H NMR spectra of crude venom from *Phlogius sp.*, *A. robustus* and *C. darlingi* recorded at 600 MHz, showing the presence of PA_{366} in the *Phlogius sp.* venom, and PA_{389} in the *A. robustus* and *C. darlingi* venom. The ^1H NMR spectra of purified PA_{366} and PA_{389} recorded at 600 MHz are also shown.

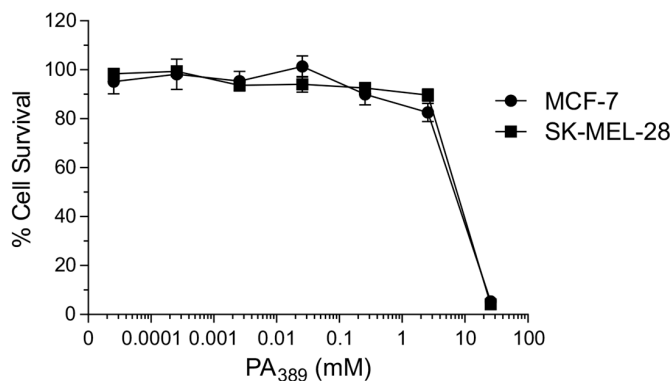


Figure 5. Cytotoxicity of PA₃₈₉ against cancer cell lines. Dose response for cytotoxic cell killing of PA₃₈₉ in MCF-7 (circles) or SK-MEL-28 (squares) cells. Cells were treated with the indicated concentrations of purified PA₃₈₉ for five days, before assay for cell survival was assessed using SRB. Cell survival percentages normalised to untreated cells are indicated. Representative data from a single experiment with triplicate readings are shown.

The venom from *H. gigas* and *N. chromatus* did not appear to contain either PA₃₆₆ or PA₃₈₉, despite displaying cytotoxic activity. *H. gigas* appears to contain primarily peptide based molecules, whereas the spectra from *N. chromatus* is dominated by small molecules but with different shifts to the polyamines characterised in this study. Comparison of the 1D spectra of *A. geniculata* and *Pamphobeteus antinous*, a tarantula species that did not display cytotoxic activity, highlights the differences in the venom NMR “profiles” in the presence and absence of small molecules, as shown in Figure 6. The NMR spectra of *A. geniculata* is dominated by PA₃₆₆, whereas *P. antinous* shows no evidence of small molecules. Instead, the venom of *P. antinous* appears to contain primarily peptides based on the large number of peaks and significant peak dispersion in the 6–9.5 ppm range. These peptides are likely to be disulfide-rich based on previous analyses of spider venoms [20].

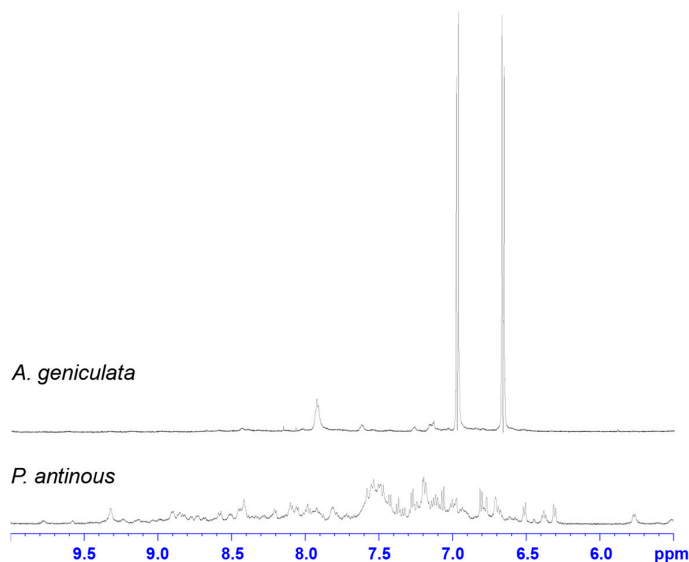


Figure 6. One-dimensional NMR spectra of selected crude spider venoms from *P. antinous* and *A. geniculata*. ¹H NMR analysis of the crude venom from *P. antinous* shows a composition that is primarily peptides, based on the number of peaks and dispersion in the amide region; this venom does not show any evidence of cytotoxicity against MCF-7, SK-MEL-28 or NFF cells. In contrast, the spectrum of cytotoxic crude venom from *A. geniculata* is dominated by the peaks corresponding to PA₃₆₆.

2.3. Protein Array Analysis

A sample of PA₃₆₆ was biotinylated for protein array analysis to identify any protein binding interactions. Biotinylated PA₃₆₆ was shown by MS analysis to have a molecular weight of 706 Da, confirming biotin binding to the primary amine at the end of the polyamine chain. Analysis of the biotinylated PA₃₆₆ binding to a human protein array demonstrated interaction with numerous proteins, presumably via non-specific interactions. Signals with Z-scores above three were considered to be significant. The polyamine bound to MAPK1 and MAP3K2; both giving Z-scores of 3.7. These proteins have previously been shown to have roles in tumour development and breast cancer [21]. The protein with the highest score however, based on the signal intensity, was a zinc finger protein (ZNF501 Z-score 13.93).

3. Discussion

In the current study, we have used NMR spectroscopy and MS to characterise the novel polyamine PA₃₆₆, which has selective cytotoxicity for MCF-7 breast cancer cells. Comparison with a related polyamine, PA₃₈₉, provided insight into the important structural features. The two polyamines consist of a spermine tail functionalised with an aromatic head group, and are identical except PA₃₆₆ has a 2-hydroxy-3-(4-hydroxyphenyl)propanal aromatic head group, while PA₃₈₉ contains a 2-hydroxy-3-(1*H*-indol-3-yl)propanal based head group. PA₃₈₉ only displays cytotoxicity at high concentrations in contrast to PA₃₆₆, indicating that the aromatic head group is important for cytotoxicity.

Using ProtoArray technology, analysis of the protein binding properties of PA₃₆₆ indicates non-specific binding to a range of proteins. However, the protein with the highest Z-score in the protein array analysis, which is likely to have the most significant interaction, is zinc finger protein 501, which belongs to the Krüppel-like c2h2 type zinc finger protein family. Zinc finger proteins are one of the most common families of DNA-binding transcription factors [22] and a recent study suggested they can be involved in tumour development [21]. Interestingly, the mammalian polyamines putrescine, spermidine and spermine alter binding of DNA to zinc finger transcription factors [23], which is consistent with a role for zinc finger protein 501 in the bioactivity of PA₃₆₆. However, additional interactions might also be involved given that MAPK1 and MAP3K2, mitogen-activated protein kinases (MAPK), were also significant hits in the ProtoArray analysis. Several MAPK genes are associated with breast cancer [24], and activation of MAPK can lead to cell proliferation, invasion and metastasis, making these kinases potential targets for cancer treatment [25,26]. To provide greater insight into the possible targets of PA₃₆₆ it is important to determine the membrane permeability, which will influence the targets accessible to the molecule.

The cytotoxicity we observed for PA₃₆₆ is consistent with the role of mammalian polyamines in cell death. Numerous links have been identified between mammalian polyamines and apoptotic pathways. For example, the production of hydrogen peroxide produced during polyamine catabolism is thought to be involved in cell death [27]. However, alteration in polyamine levels can have an impact on numerous cellular functions such as DNA-protein interactions, protein-protein interactions and mitochondrial integrity which can lead to cell death. Morphological analysis of the cells following incubation with PA₃₆₆ indicates the presence of apoptosis but further study is required to confirm this hypothesis.

Although PA₃₆₆ displays cytotoxicity against a cancer cell lines, this is unlikely to be related to its function in the spider venom. The primary target of venom polyamine toxins is thought to be the ionotropic glutamate receptors [28]. PA₃₈₉ has previously been shown to cause rapid but reversible paralysis to lepidopteran insect larvae, suggesting a role in prey capture [19]. Given the structural and functional similarities between PA₃₈₉ and PA₃₆₆, it is likely that the latter also displays some form of bioactivity against insect prey.

The known distribution of PA₃₆₆ and PA₃₈₉ determined from previous work and this study is shown in the phylogenetic tree in Figure 7. PA₃₆₆ is present in a range of geographically diverse spider

species from the family Theraphosidae, indicating that differences such as diet and environmental conditions are unlikely to influence the production of this polyamine. Similarly, PA₃₈₉ is present in the venom of spiders from the Theraphosidae family, but also in the venom of species from the Hexathelidae and Ctenizidae families. In this study, we have confirmed the presence of PA₃₈₉ in the venom of the Sydney Funnel-web spider, *Atrax robustus*, as the undefined 3-(3-indoyl)lactic acid and spermine complex suggested by Sutherland [29] and proposed as identical to PA₃₈₉ by Skinner et al. [19]. It is likely that PA₃₆₆ is also present in other spider families but further analysis is required to confirm this hypothesis.

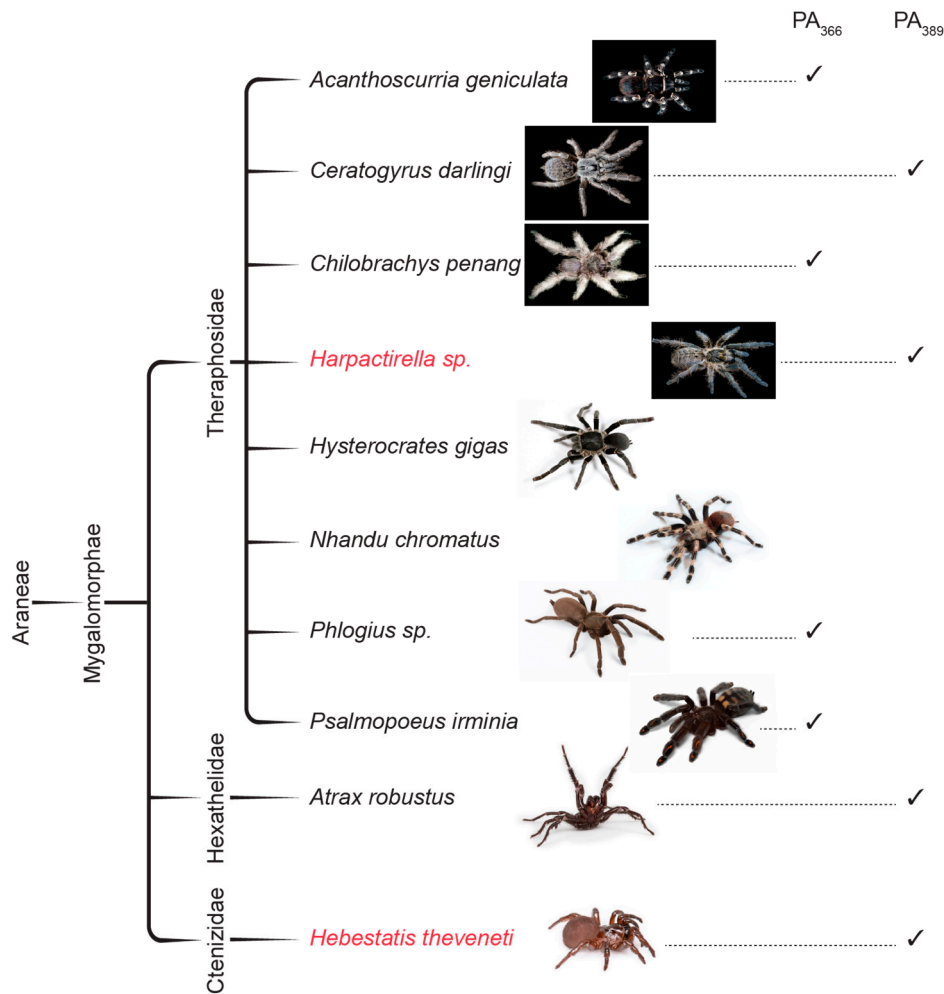


Figure 7. Phylogenetic tree of some spider venoms showing the distribution of PA₃₆₆ and PA₃₈₉. A phylogenetic tree of crude spider venoms that demonstrated cytotoxicity on MCF-7 or SK-MEL-28 cells in this study, and the presence of the polyamines PA₃₆₆ and PA₃₈₉. The two spider species, *Hebestatis theveneti* and *Harpactirella sp.*, from the original identification and characterisation study of PA₃₈₉ are also included [19] (Photograph credits: *Acanthoscurria geniculata*, *Ceratogyrus darlingi*, *Harpactirella sp.*, *Hysteroocrates gigas*, and *Nhandu chromatus*—Bastian Rast; *Chilobrachys penang*—Muhammad Ashraf; *Psalmopoeus irminia*—Edward Evans; *Hebestatis theveneti*—Marshal Hedin; *Phlogius sp.* and *Atrax robustus*—David Wilson).

One outcome of this study is NMR spectroscopy proved an effective way of screening and detecting the presence of the polyamines PA₃₆₆ and PA₃₈₉ without the need for fractionation of the venom. Although the spider venoms contain a large number of disulfide-rich peptides, the polyamines have low molecular weights and provide much sharper spectral peaks, and can be detected when only low microgram amounts of material are present in contrast to the larger peptides. This type

of NMR spectroscopy screening has also been shown to be useful for the discovery of new small molecules from other sources. For example, unfractionated extracts from insects examined using 2D NMR spectroscopy led to the discovery of tricyclic pyrones from a ladybird beetle including the identification of ring systems that had not previously been found in nature [1].

Despite the conservation of PA₃₆₆ in several venoms, our study also serves to highlight the compound diversity and broad range of biological activities found in spider venom. *N. chromatatus* has early eluting peaks from RP-HPLC that display cytotoxicity but the venom does not appear to contain PA₃₆₆ or PA₃₈₉. The 1D NMR spectrum indicates the presence of small molecules, and it is likely there are several, related polyamines that might account for our observed activity. Although there is evidence of small molecules in the crude venom of *H. gigas*, the venom is dominated by peptides/proteins in contrast to the venoms such as *Phlogius* sp., *A. robustus* and *C darlingi*. Furthermore, *P. antinous* appears to show only peptide related peaks in the amide region, and does not display cytotoxicity. This compound and bioactivity diversity is one of the features that has led to the extensive study of spider venom for the discovery of novel compounds for therapeutic or agricultural applications [20].

In summary, we have shown that a spider venom polyamine can have relatively selective cytotoxicity activity against specific cancer cell lines and that the aromatic head group appears to be involved in conferring cytotoxicity. Insight into the distribution of spider venom polyamines across species and genera has also been gained from screening using NMR spectroscopy.

4. Materials and Methods

4.1. Venom Collection and Purification

A majority of the crude venoms were purchased from the commercial supplier Alphabiotoxine Laboratory, Montroeuil-au-bois, Hainaut, Belgium. Crude venom from *Pterinochilus meridionalis*, *Vitalius roseus* and *Hogna carolinensis* was purchased from SpiderPharm, Yarnell, AZ, USA. Crude venom was also collected from a colony of housed specimens of female Australian tarantulas (*Phlogius* sp. and *Coremiocnemis tropix*), *Macrothele gigas*, and *Poecilotheria fasciata* and *Poecilotheria metallica* by electrostimulation of the venom glands. Male Sydney funnel-web spider (*Atrax robustus*) venom (~5 mg) was supplied by the Australian Reptile Park (Gosford, NSW, Australia). Crude venom was fractionated by reversed-phase HPLC (RP-HPLC) using an Agilent 1260 Infinity HPLC system (Agilent, Santa Clara, CA, USA) and a Thermo Scientific Hypersil GOLD aQ (250 × 10 mm, 5 µm) column (Thermo Fisher Scientific, Waltham, MA, USA). Fractionation of the venom components was achieved using a linear gradient of two mobile phases: H₂O/0.05% trifluoroacetic acid (TFA; Auspep, Tullamarine, VIC, Australia) [solvent A], and 90% acetonitrile (ACN; Sigma-Aldrich, St. Louis, MO, USA)/H₂O/0.045% TFA [solvent B]. Separation used a gradient of 5–80% solvent B in 75 min, 80–90% solvent B in 5 min, 90% solvent B for 5 min, and 90–5% solvent B in 2 min at a flow rate of 6 mL/min. Venom component elution was monitored at 214 nm and 1 min fractions were collected.

4.2. Cytotoxicity Assays

All cells were cultured in RPMI-1640 medium supplemented with 10% heat-inactivated foetal calf serum (Life Technologies, Carlsbad, CA, USA) in RPMI-1640 medium supplemented with 100 U/mL penicillin, 100 µg/mL streptomycin, and 3 mM HEPES at 5% CO₂, 99% humidity at 37 °C. Routine mycoplasma tests were performed using Hoechst stain or PCR and were always negative. The cytotoxicity of compounds was determined using clonogenic survival assays of MCF-7 (breast adenocarcinoma), SK-MEL-28 (melanoma) and human neonatal foreskin fibroblasts (NFF) cells [30,31]. The cell lines were purchased from ATCC. Cells were plated into 96-well microtitre plates at 5 × 10³ cells/well, and allowed to adhere overnight. Compounds were added to culture medium at the indicated final concentrations, and plates incubated under the above conditions for five days. Cell survival was then assayed using sulforhodamine B (SRB; Sigma, St. Louis, MO, USA). Briefly, the culture medium was removed from the 96-well microtitre plates and the plates washed

twice with phosphate buffered saline (PBS), before the cells were fixed with methylated spirits for 15 min. The plates were then rinsed with tap water and the fixed cells stained with 50 μL /well of SRB solution (0.4% sulforhodamine B (*w/v*) in 1% (*v/v*) acetic acid) over a period of 1 h. The SRB solution was removed from the wells and the plates rapidly washed two times with 1% (*v/v*) acetic acid. Protein bound dye was then solubilised with the addition of 100 μL of 10 mM unbuffered Tris, and incubated for 15 min at 25 $^{\circ}\text{C}$. Plates were then read at 564 nm on a VERSA max tuneable microplate reader (Molecular Devices, Sunnyvale, CA, USA). Negative (vehicle only) and positive (cisplatin) controls were run with every cell survival experiment to ensure the quality of the data. Vehicle only control results in <5% change in cell survival whereas the positive control inhibited cell survival at nanomolar concentrations as expected.

4.3. Mass Spectrometry and NMR Analysis

^1H NMR and ^{13}C NMR spectra were recorded at 600.13 MHz and 150.91 MHz at 298 K on a Bruker Avance III 600 MHz spectrometer (Bruker, Billerica, MA, USA) equipped with a cryoprobe. Samples were dissolved in 90% H_2O /10% D_2O (*v/v*) (100 μM). D_2O (99.9%) was obtained from Cambridge Isotope Laboratories, Woburn, MA, USA for ^1H NMR measurements. Spectra were referenced to 4,4-dimethyl-4-silapentane-1-sulfonic acid (DSS; Cambridge Isotope Laboratories, Woburn, MA, USA). Two-dimensional spectra included TOCSY, NOESY, DQF-COSY, HSQC, HMBC and HSQC-TOCSY. TOCSY and NOESY mixing times of 80 ms and 500 ms respectively were used. Spectra were analyzed using TOPSPIN (Bruker, Billerica, MA, USA).

Mass spectrometry (MS) was performed using a SCIEX TOF/TOFTM 5800 MALDI, and high resolution mass spectrometry (HRMS) using direct infusion on a SCIEX QSTAR Elite equipped with a nanospray (SCIEX, Framingham, MA, USA). MALDI-MS samples were spotted on 384-well stainless steel target plates using 0.5 μL of sample and 0.5 μL of either α -cyano-4-hydroxycinnamic acid (CHCA; Sigma-Aldrich, St. Louis, MO, USA) matrix at 7.5 mg/mL in 50% ACN/0.1% TFA, or 2,5-dihydroxybenzoic acid (DHB; Sigma-Aldrich, St. Louis, MO, USA) matrix at 10 mg/mL in 50% ethanol/0.1% TFA. Calibration was performed before spectra collection for each sample using Calibration Mix solution 2 (SCIEX, Framingham, MA, USA). Spectra were acquired in reflector positive ion mode from m/z 300 to 1000 Da, and averaged over 2000 laser shots. QSTAR Elite MS samples were infused at 2 $\mu\text{L}/\text{min}$. MS spectra were acquired in positive ion mode from m/z 200 to 1000 Da and spectra were externally calibrated using SCIEX renin standard. MS/MS spectra were acquired for the product ions 367.26 Da and 390.2 Da from m/z 10 to 500 Da. All spectra were acquired with an accumulation time of 1 s, using an ion-spray voltage of 3700 V, a declustering potential of 80 V, and a focussing potential of 280 V.

4.4. Protein Array Analysis

Biotinylation of PA₃₆₆ for protein interaction analysis was achieved utilising a 20-fold excess of EZ-Link[®] Sulfo-NHS-LC-biotin (ThermoFisher Scientific, Waltham, MA, USA), and following the manufacturer's instructions. Successful labelling of PA₃₆₆ was confirmed by molecular weight analysis using a SCIEX TOF/TOFTM 5800 mass spectrometer (SCIEX, Framingham, MA, USA), followed by RP-HPLC purification of labelled PA₃₆₆ to remove excess non-reacted and hydrolyzed biotin reagent from the solution. The purified sample was dried and resuspended in 100 μL of 1.0% PBS (pH 7.2) to achieve a required final amount of 10 μg . Interactions between biotinylated PA₃₆₆ and more than 9000 human proteins were investigated employing a ProtoArray[®] Human Protein Microarray v5.0 Protein-Protein Interaction (PPI) kit (InvitrogenTM, Carlsbad, CA, USA), and significant interactions detected using a GenePix[®] 4000B microarray scanner (Molecular Devices, Sunnyvale, CA, USA), according to the manufacturer's instructions.

Supplementary Materials: The following are available online at <http://www.mdpi.com/2072-6651/9/11/346/s1>.
Table S1: Crude spider venoms tested for cytotoxicity against MCF-7 cells.

Acknowledgments: This work was funded in part by a grant from the National Breast Cancer Foundation (D.W., G.M.B., P.G.P., L.D.R., N.L.D.). Fellowship support was provided to AL from NHMRC (1020114) and N.L.D. from the Australian Research Council (FF110100226). The authors are grateful to Volker Herzig (I.M.B., Q.L.D.) for providing crude venom from *Macrothele gigas*, *Coremiocnemis tropix*, *Poecilotheria fasciata*, and *Poecilotheria metallica*, the Australian Reptile Park (Gosford, NSW) for the provision of crude male Sydney funnel-web spider venom, and to Bastian Rast, Edward Evans, Marshal Hedin, and Muhammad Ashraf for the provision of photographs.

Author Contributions: D.W., L.D.R., and N.L.D. designed the study. D.W., G.M.B., L.M., M.J.N., P.G.P., J.J.S., L.T., A.L., M.J.L., L.D.R., and N.L.D. carried out experiments. D.W. and N.L.D. wrote the paper. All authors analysed the results and approved the final version of the manuscript.

Conflicts of Interest: The authors declare no conflict of interest.

References

1. Deyrup, S.T.; Eckman, L.E.; McCarthy, P.H.; Smedley, S.R.; Meinwald, J.; Schroeder, F.C. 2D NMR-spectroscopic screening reveals polyketides in ladybugs. *Proc. Natl. Acad. Sci. USA* **2011**, *108*, 9753–9758. [[CrossRef](#)] [[PubMed](#)]
2. Shanmugam, M.K.; Lee, J.H.; Chai, E.Z.; Kanchi, M.M.; Kar, S.; Arfuso, F.; Dharmarajan, A.; Kumar, A.P.; Ramar, P.S.; Looi, C.Y.; et al. Cancer prevention and therapy through the modulation of transcription factors by bioactive natural compounds. *Semin. Cancer Biol.* **2016**, *40–41*, 35–47. [[CrossRef](#)] [[PubMed](#)]
3. Doroghazi, J.R.; Albright, J.C.; Goering, A.W.; Ju, K.S.; Haines, R.R.; Tchalukov, K.A.; Labeda, D.P.; Kelleher, N.L.; Metcalf, W.W. A roadmap for natural product discovery based on large-scale genomics and metabolomics. *Nat. Chem. Biol.* **2014**, *10*, 963–968. [[CrossRef](#)] [[PubMed](#)]
4. Wickenden, A.; Priest, B.; Erdemli, G. Ion channel drug discovery: Challenges and future directions. *Future Med. Chem.* **2012**, *4*, 661–679. [[CrossRef](#)] [[PubMed](#)]
5. Escoubas, P.; Sollod, B.; King, G.F. Venom landscapes: Mining the complexity of spider venoms via a combined cDNA and mass spectrometric approach. *Toxicon* **2006**, *47*, 650–663. [[CrossRef](#)] [[PubMed](#)]
6. World Spider Catalog v18.0. Available online: <http://www.wsc.nmbe.ch/> (accessed on 10 April 2017).
7. Saez, N.J.; Senff, S.; Jensen, J.E.; Er, S.Y.; Herzig, V.; Rash, L.D.; King, G.F. Spider-venom peptides as therapeutics. *Toxins (Basel)* **2010**, *2*, 2851–2871. [[CrossRef](#)] [[PubMed](#)]
8. Schroeder, F.C.; Taggi, A.E.; Gronquist, M.; Malik, R.U.; Grant, J.B.; Eisner, T.; Meinwald, J. NMR-spectroscopic screening of spider venom reveals sulfated nucleosides as major components for the brown recluse and related species. *Proc. Natl. Acad. Sci. USA* **2008**, *105*, 14283–14287. [[CrossRef](#)] [[PubMed](#)]
9. Mortari, M.R.; Cunha, A.O.; Ferreira, L.B.; dos Santos, W.F. Neurotoxins from invertebrates as anticonvulsants: From basic research to therapeutic application. *Pharmacol. Ther.* **2007**, *114*, 171–183. [[CrossRef](#)] [[PubMed](#)]
10. Rhee, H.J.; Kim, E.J.; Lee, J.K. Physiological polyamines: Simple primordial stress molecules. *J. Cell. Mol. Med.* **2007**, *11*, 685–703. [[CrossRef](#)] [[PubMed](#)]
11. Linsalata, M.; Orlando, A.; Russo, F. Pharmacological and dietary agents for colorectal cancer chemoprevention: Effects on polyamine metabolism (review). *Int. J. Oncol.* **2014**, *45*, 1802–1812. [[CrossRef](#)] [[PubMed](#)]
12. Stromgaard, K.; Jensen, L.S.; Vogensen, S.B. Polyamine toxins: Development of selective ligands for ionotropic receptors. *Toxicon* **2005**, *45*, 249–254. [[CrossRef](#)] [[PubMed](#)]
13. Davis, R.A.; Vullo, D.; Supuran, C.T.; Poulsen, S.A. Natural product polyamines that inhibit human carbonic anhydrases. *Biomed. Res. Int.* **2014**, *2014*, 374079. [[CrossRef](#)] [[PubMed](#)]
14. Kostopoulou, O.N.; Kouvela, E.C.; Magoulas, G.E.; Garnelis, T.; Panagoulas, I.; Rodi, M.; Papadopoulos, G.; Mouzaki, A.; Dinos, G.P.; Papaioannou, D.; et al. Conjugation with polyamines enhances the antibacterial and anticancer activity of chloramphenicol. *Nucleic Acids Res.* **2014**, *42*, 8621–8634. [[CrossRef](#)] [[PubMed](#)]
15. Quistad, G.B.; Suwanrumpha, S.; Jarema, M.A.; Shapiro, M.J.; Skinner, W.S.; Jamieson, G.C.; Lui, A.; Fu, E.W. Structures of paralytic acylpolyamines from the spider *Agelenopsis aperta*. *Biochem. Biophys. Res. Commun.* **1990**, *169*, 51–56. [[CrossRef](#)]

16. Traynelis, S.F.; Wollmuth, L.P.; McBain, C.J.; Menniti, F.S.; Vance, K.M.; Ogden, K.K.; Hansen, K.B.; Yuan, H.; Myers, S.J.; Dingledine, R. Glutamate receptor ion channels: Structure, regulation, and function. *Pharmacol. Rev.* **2010**, *62*, 405–496. [[CrossRef](#)] [[PubMed](#)]
17. Wilson, D.; Alewood, P.F. Taxonomy of australian funnel-web spiders using rp-hplc/esi-ms profiling techniques. *Toxicon* **2006**, *47*, 614–627. [[CrossRef](#)] [[PubMed](#)]
18. Tzouros, M.; Chesnov, S.; Bigler, L.; Bienz, S. A template approach for the characterization of linear polyamines and derivatives in spider venom. *Eur. J. Mass Spectrom. (Chichester)* **2013**, *19*, 57–69. [[CrossRef](#)]
19. Skinner, W.S.; Dennis, P.A.; Lui, A.; Carney, R.L.; Quistad, G.B. Chemical characterization of acylpolyamine toxins from venom of a trap-door spider and two tarantulas. *Toxicon* **1990**, *28*, 541–546. [[CrossRef](#)]
20. Pineda, S.S.; Undheim, E.A.; Rupasinghe, D.B.; Ikonopoulou, M.P.; King, G.F. Spider venomics: Implications for drug discovery. *Future Med. Chem.* **2014**, *6*, 1699–1714. [[CrossRef](#)] [[PubMed](#)]
21. Tan, Z.; Zhang, S.; Li, M.; Wu, X.; Weng, H.; Ding, Q.; Cao, Y.; Bao, R.; Shu, Y.; Mu, J.; et al. Regulation of cell proliferation and migration in gallbladder cancer by zinc finger x-chromosomal protein. *Gene* **2013**, *528*, 261–266. [[CrossRef](#)] [[PubMed](#)]
22. Lodomery, M.; Dellaire, G. Multifunctional zinc finger proteins in development and disease. *Ann. Hum. Genet.* **2002**, *66*, 331–342. [[CrossRef](#)] [[PubMed](#)]
23. Thomas, T.; Kiang, D.T. Modulation of the binding of progesterone receptor to DNA by polyamines. *Cancer Res.* **1988**, *48*, 1217–1222. [[PubMed](#)]
24. Slattery, M.L.; Lundgreen, A.; John, E.M.; Torres-Mejia, G.; Hines, L.; Giuliano, A.R.; Baumgartner, K.B.; Stern, M.C.; Wolff, R.K. Mapk genes interact with diet and lifestyle factors to alter risk of breast cancer: The breast cancer health disparities study. *Nutr. Cancer* **2015**, *67*, 292–304. [[CrossRef](#)] [[PubMed](#)]
25. Zhao, M.; Ramaswamy, B. Mechanisms and therapeutic advances in the management of endocrine-resistant breast cancer. *World J. Clin. Oncol.* **2014**, *5*, 248–262. [[CrossRef](#)] [[PubMed](#)]
26. Jiang, K.; Lu, Q.; Li, Q.; Ji, Y.; Chen, W.; Xue, X. Astragaloside iv inhibits breast cancer cell invasion by suppressing vav3 mediated rac1/mapk signaling. *Int. Immunopharmacol.* **2017**, *42*, 195–202. [[CrossRef](#)] [[PubMed](#)]
27. Thomas, T.; Thomas, T.J. Polyamines in cell growth and cell death: Molecular mechanisms and therapeutic applications. *Cell. Mol. Life Sci.* **2001**, *58*, 244–258. [[CrossRef](#)] [[PubMed](#)]
28. Mellor, I.R.; Usherwood, P.N. Targeting ionotropic receptors with polyamine-containing toxins. *Toxicon* **2004**, *43*, 493–508. [[CrossRef](#)] [[PubMed](#)]
29. Sutherland, S.K. Isolation, mode of action and properties of the major toxin (atrazotoxin) in the venom of the sydney funnel web spider (*atraz robustus*). *Proc. Aust. Soc. Med. Res.* **1973**, *3*, 172.
30. Ogbourne, S.M.; Suhrbier, A.; Jones, B.; Cozzi, S.J.; Boyle, G.M.; Morris, M.; McAlpine, D.; Johns, J.; Scott, T.M.; Sutherland, K.P.; et al. Antitumor activity of 3-ingenyl angelate: Plasma membrane and mitochondrial disruption and necrotic cell death. *Cancer Res.* **2004**, *64*, 2833–2839. [[CrossRef](#)] [[PubMed](#)]
31. Cozzi, S.J.; Parsons, P.G.; Ogbourne, S.M.; Pedley, J.; Boyle, G.M. Induction of senescence in diterpene ester-treated melanoma cells via protein kinase c-dependent hyperactivation of the mitogen-activated protein kinase pathway. *Cancer Res.* **2006**, *66*, 10083–10091. [[CrossRef](#)] [[PubMed](#)]

